Gas phase Photoemission studies in the hard X-ray domain

Marc Simon[1*]

[1]Sorbonne Université, CNRS, Laboratoire de Chimie Physique-Matière et Rayonnement, LCPMR, 75005 Paris, France

Abstract. Recent results obtained in gas phase photoemission studies are presented in this article with particular emphasis on recoil, Double Core Hole and Post Collision Interaction. These three important effects are not specific to the gas phase and could have more general applications in condensed matter studies.

1 Introduction

Light-Matter interaction studied by photoemission on gas phase samples has proven to furnish a wealth of information. This article deals with Hard X-ray Photoelectron Spectroscopy (HAXPES) with a focus on the tender x-ray domain (2-12 keV). One of the interests of this photon energy range is the short (femtosecond or less) core-hole lifetime of the reached electronic states by photoabsorption. Among the different studies performed by our group, I will select three important fundamental processes, which could attract the condensed phase community participating in the JNSPE: high recoil effects due to the high kinetic energy of the emitted photoelectron, Double Core Hole Spectroscopy and Post Collision Interaction. These studies have important applications like radiation-damage in the hard x-ray domain. The measurements were performed at SOLEIL, the French Synchrotron facility, located close to Paris. The perspectives offered by these results are discussed. We have published several review articles in the past where the reader could find more details [1-3].

2 Experimental setup

The HAXPES experimental chamber is a permanent endstation of the SOLEIL GALAXIES beamline.

2.1 The SOLEIL GALAXIES beamline

The GALAXIES beamline is an undulator beamline, optimized to operate in the 2-12 keV energy range [4]. The undulator beam is monochromatized by a double-crystal monochromator providing a photon flux of few 10^{12} photons per second on the sample. A 4-bounce, high-resolution monochromator (HRM) has been recently commissioned allowing to obtain a photon bandwidth of 100 meV between 4 and 12 keV.

2.2 The HAXPES endstation

HAXPES is a permanent endstation of the GALAXIES beamline [5]. A high-resolution hemispherical electron analyzer allows to measure electron spectra with a kinetic energy resolution of 35 meV for electron kinetic energies up to 12 keV. For gas phase studies, a gas cell is installed into the photon beam thanks to a motorized 4-axes manipulator.

*Corresponding author: marc.simon@sorbonne-universite.fr. ORCID: https://orcid.org/0000-0002-2525-5435

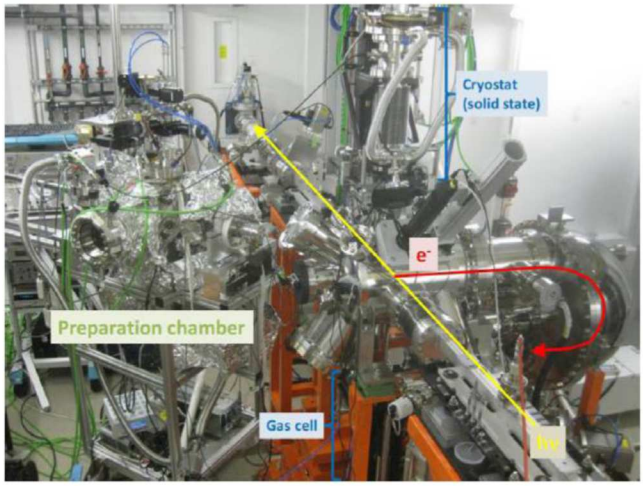

Fig. 1. Photo of the HAXPES endstation of the SOLEIL GALAXIES beamline.

3 Recoil effects

In the hard x-ray domain, the momentum of the departing photoelectron is far to be negligeable as it is the case in the soft x-ray domain. This leads to translational recoil for isolated atoms and molecules. Additionally, depending on the direction in which the photoelectron is ejected, vibrational and rotational recoil have been observed for molecules.

3.1 Translational recoil

Core ionization of neon has been studied as a demonstration case [6]. Ne1s ionization has been performed at high photon energy and the Auger electrons have been measured for different photon energies. The recoil momentum of the Ne^+ ion is so high that Atomic Auger Doppler effects have been observed, as illustrated in figure 2.

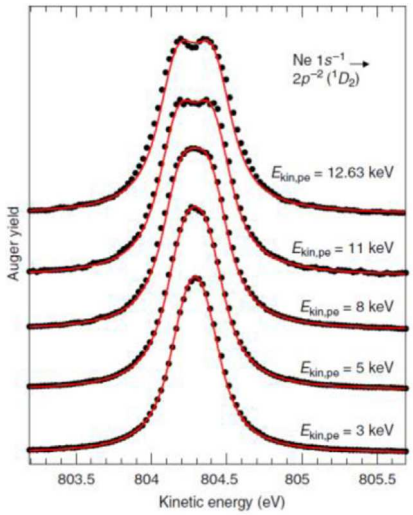

Fig. 2. Atomic Auger Doppler effects of core-ionized neon at various kinetic energy of the 1s photoelectron.

3.2 Vibrational recoil

In the case of carbon 1s photoionization of the CF_4 molecule, the escaping C1s photoelectron cannot induce rotational recoil of the CF_4^+ ion because the carbon atom is located at the center of gravity of the tetrahedral molecule. In addition to the translational recoil, only vibrational recoil is then induced by the fast C1s photoelectron emission, as illustrated in figure 3 [7]. Close to the C1s Photoionization threshold, only a single

vibrational level of the CF_4^+ ion is populated. When the photon energy is increased, a wider vibrational envelope is observed as a signature of the vibrational recoil.

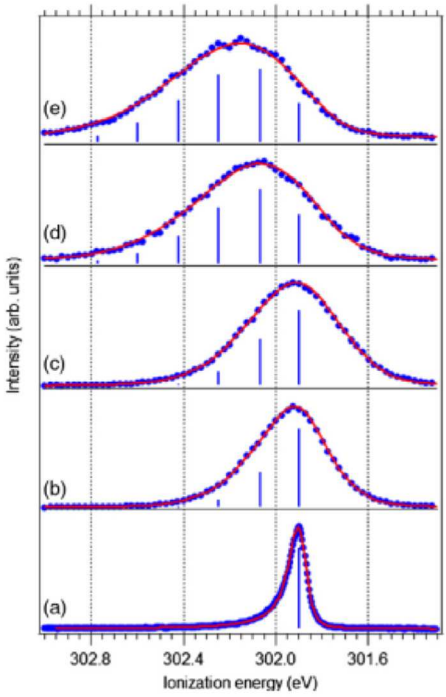

Fig. 3. Vibrational recoil of the C1s core-ionized CF_4 molecule measured at different photon energies.

3.3 Rotational recoil

In case of the CO molecule, C1s photoionization can lead to vibrational recoil if the photoelectron is emitted parallel to the molecular axis and to rotational recoil if the photoelectron is emitted perpendicular to the molecular axis. Rotational levels cannot be resolved at such high kinetic energies. Rotational recoil effects are observed as a shift of the centroid of the photoelectron peak toward lower kinetic energy, the difference in energy being the rotational energy of the molecular ion. This rotational recoil has been precisely determined by a mixture of CF_4 and CO molecules as illustrated in figure 4.

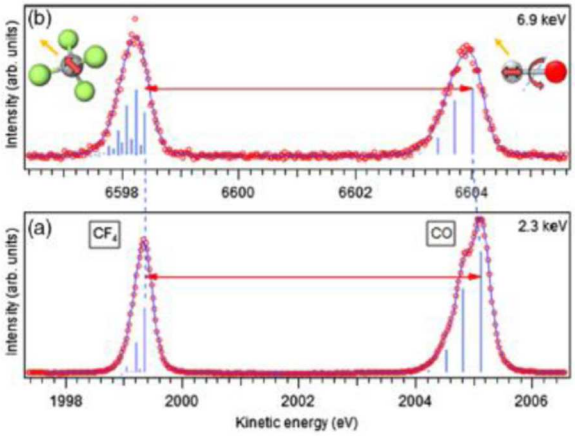

Fig. 4. C1s photoelectron of a mixture of CF_4 and CO molecule. Arrows are showing the kinetic energy difference between the v=0 of both molecular ions which vary with the upcoming photon energy due to the rotational recoil.

3.4 Recoil induced ultrafast molecular rotation of the CO molecule probed by dynamical rotational Doppler effect

Photoionization at high photon energy induces ultra-fast rotation up to an effective rotational temperature of about 10,000 K due to the recoil caused by emission of a fast photoelectron. In order to monitor the recoil-induced rotational motion of the CO molecule, high-resolution Auger spectra of the C1s core-ionized molecular ion have been recorded at various photon energies [8]. Given the C1s core-hole lifetime, the molecular ion has a time of 5 femtoseconds to rotate before the Auger electron emission. This is illustrated in figure 5.

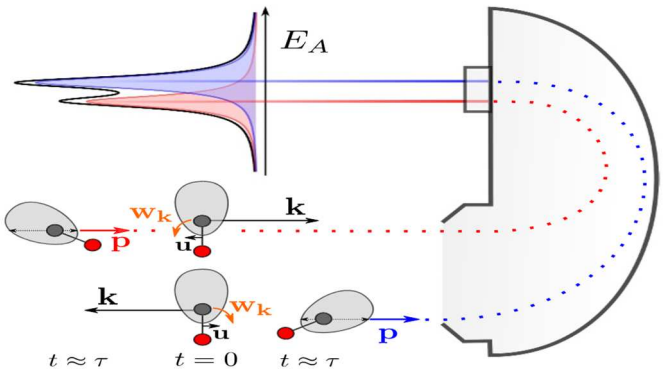

Fig. 5. Classical picture of the dynamical rotational Doppler effect of the C1s core-ionized CO molecule

4 Double Core Hole Spectroscopy

Double Core Hole (DCH) studies are attract considerable interest mainly because of the high chemical sensitivity of the DCH binding energy compared to the traditional ESCA (Electron Spectroscopy for Chemical Analysis) technique [9]. In case of ESCA, a chemical shift of 700 meV has been recently measured between the CH_3I and CF_3I molecules at the iodine 1s ionization threshold around 33 keV binding energy [10]. These results have been obtained at the Spring8 synchrotron radiation facility where an HAXPES endstation has been successfully commissioned in the hard x-ray domain [11]. The high sensitivity of DCH states has been theoretically predicted during the 1980's and but only experimentally confirmed very recently [12]. Most of the DCH studies have used sophisticated magnetic bottles in order to measure both core-ionized photoelectrons in a coincidence regime. An interesting way to study DCH states has been recently founded [13]: one of the core electrons is ejected into the continuum whereas a second core electron is promoted to an empty molecular orbital.

4.1 Spectroscopy of DCH states

The high-resolution of the HAXPES setup is particularly well adapted to perform DCH studies with one core electron ionized and the other promoted into an unoccupied level. A proof of principle has been performed with the argon $1s^{-1}2p^{-1}$ shake-up photoelectron spectrum shown figure 6 [14]. The Rydberg series of the DCH states converging towards the $^3P_2$, $^3P_1$, $^3P_0$ and $^1P_1$ DCH thresholds are clearly visible with a good signal/noise ratio. Spectral bandwidth has been measured allowing to determine the lifetime of the DCH states.

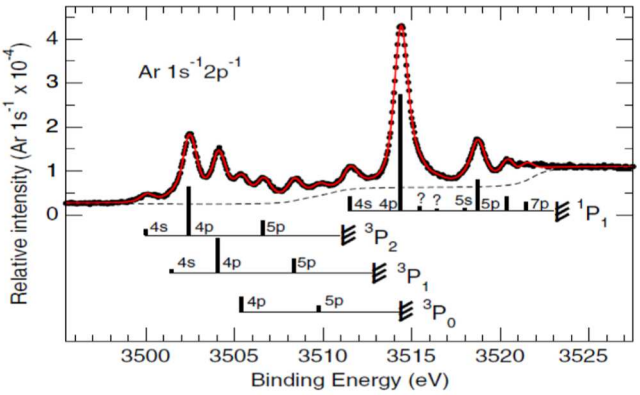

Fig. 6. $1s^{-1}2p^{-1}$ DCH shake-up photoelectron spectrum of argon

This technique has been applied to the neon atom [15], the H_2O molecule [16], the CS_2 and SF_6 molecules [17], the HCl molecule [18], the O K^{-2} CO_2 molecule [19].

4.2 Electronic relaxation of DCH states

The Auger relaxation of these DCH states mainly occurs via a 2 step Auger decay: a first Auger decay filling one core hole of the DCH state, called hypersatellite Auger decay, occurs followed by a second Auger decay filling the remaining core hole. Even if the relative ratio of DCH/SCH states is in the order of 10^{-3}, good signal/noise ratio spectra have been obtained on neon [15, 20] as illustrated in figure 7.

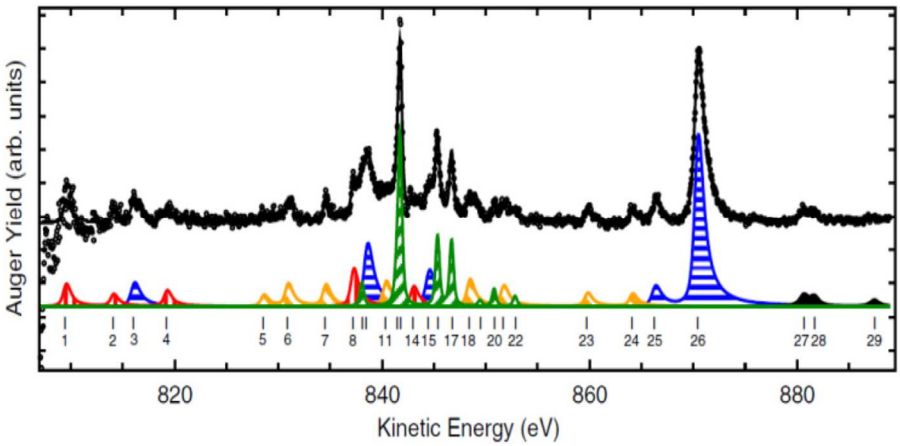

Fig. 7. Hypersatellite Auger spectrum of neon.

The relaxation of these DCH states mainly occurs via a 2 step Auger decay: a first Auger decay filling one core hole of the DCH state, called hypersatellite Auger decay, occurs followed by a second Auger decay filling the remaining core hole. Even if the relative cross section of DCH/SCH states is in the order of 10^{-3}, nice signal/noise ratio spectra have been obtained.

The hypersatellite Auger spectrum of the H_2O molecule has revealed [21] ultra-fast nuclear motion occurring within the lifetime of the DCH state which is equal to 1.5 femtosecond.

4.3 DCH states studies through cascade Auger decay

Deep shell excitation leads to cascade Auger decay. Resonant KLL Auger decay after resonant K shell excitation of the HCl molecule have revealed ultra-fast fragmentation of the HCl^+ ion prior to the Auger decay of the L^{-2}DCH

state [22-23] as illustrated in figure 8. The gradient of the Potential Energy Curve is so strong that the wave packet propagation has time to propagate during the 3 femtoseconds lifetime of the L^{-2} DCH state.

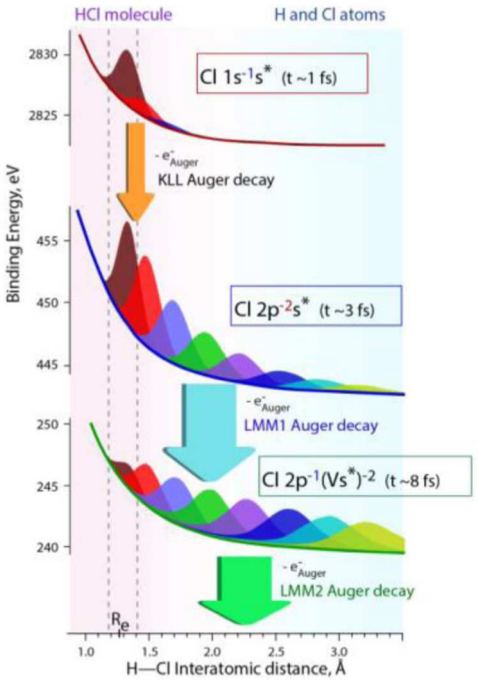

Fig. 8. Potential energy curves for different steps of the KLL Auger cascade following Cl $1s \rightarrow \sigma^*$ excitation of the HCl molecule.

Complementary Resonant Auger and Resonant X-ray emission measurements allowed to determine the lifetime of the DCH state and the gradient of the Potential Energy curve of the CH_3I molecule [24].

5 Post Collision Interaction (PCI)

Post Collision Interaction (PCI) effect takes place in presence of a slow photoelectron and a fast Auger electron. Close to the ionization threshold, the slow photoelectron starts to leave a singly charged ion, but then the faster Auger electron overtakes it. Then, instead of "feeling" the potential of a singly charged ion, the photoelectron suddenly 'feels' a doubly charged ion. Due to PCI, the photoelectron loses kinetic energy and the Auger electron simultaneously gains kinetic energy [25-27]. Just above threshold, the photoelectron can be recaptured into a unoccupied Rydberg orbital. Momentum transfer between the slow photoelectron and the fast Auger electron can also takes place [28].

PCI is a quite general effect. Several groups are working for the moment on PCI on liquids and solid states compounds.

6 Conclusion

All the presented effects presented in this overview have been observed in the gas phase during the last ten years. Recoil, Double Core Hole and PCI are easier to observe with diluted species but can be studied in any phases.

Acknowledgements

I warmly acknowledge all the coauthors of the presented articles and particularly Maria Novella Piancastelli, Oksana Travnikova, Tatiana Marchenko, Renaud Guillemin, Iyas Ismail, Ralph Püttner and Denis Céolin.

References

1. M. Simon, M. N. Piancastelli and D. W. Lindle *Hard X-Ray Photoelectron Spectroscopy from Atoms and Molecules (HAXPES)* (*Springer Series in Surface Science* vol 59) ed J. Woicik (New York: Springer) (2016)
2. M. N. Piancastelli et al., J. Phys. B 50 042001 (2017)
3. M. N. Piancastelli et al., Rep. Prog. Phys. 83 016401 (2020)
4. J.-P. Rueff et al., J. Synchrotron Radiation 22 175 (2015)
5. D. Céolin et al., J. Electron Spectrosc. and Relat. Phenom. 190 188 (2013)
6. M. Simon et al., Nature Communications 5 4069 (2014)
7. E. Kukk et al., Phys. Rev. Lett. 121 073002 (2018)
8. D. Céolin et al., Proceedings of the National Academy of Sciences 116 4877 (2019)
9. L. Cederbaum et al., J. Chem. Phys. 85 6513 (1986)
10. N. Boudjemia et al., Phys. Chem. Chem. Phys. 21 5448 (2019)
11. M. Oura et al., New J. Phys. 21 043015 (2019)
12. D. Koulentianos et al., J. Chem. Phys. 149, 134313 (2018)
13. M. Nakano et al., Phys. Rev. Lett. 111 123001 (2013)
14. R. Püttner et al., Phys. Rev. Letters, 114, 093001 (2015)
15. G. Goldsztejn et al., Phys. Rev. Letters 117, 133001 (2016)
16. T. Marchenko et al., J. Physics B 53 224002 (2021)
17. R. Feifel et al., Scientific Reports 7 13317 (2017)
18. D. Koulentianos et al., Phys. Chem. Chem. Phys. 20, 2724 (2018)
19. D. Koulentianos et al., Phys. Chem. Chem. Phys. 23, 10780 (2021)
20. G. Goldsztejn et al., Phys. Rev. A 96 012513 (2017)
21. T. Marchenko et al., Phys. Rev. A 98 063403 (2018)
22. O. Travnikova et al., Physical Review Letters116, 213001 (2016)
23. O. Travnikova et al., Physical Review Letters 118, 213001 (2017)
24. T. Marchenko et al., Physical Review Letters 119, 133001 (2017)
25. R. Guillemin et al., Physical Review Letters 109, 013001 (2012)
26. R. Guillemin et al., Physical Review A 92, 012503 (2015)
27. S. Kosugi et al., Physical Review Letters 124, 183001 (2020)
28. R. Guillemin et al., Physical Review A 99, 063409 (2019)